J. of Electromagn. Waves and Appl., Vol. 17, No. 1, 79–98, 2003

MODAL NEAR-FIELD TO FAR-FIELD TRANSFORMATION FOR FDTD MODELLING OF APERTURE ANTENNAS

G. Marrocco

Dipartimento di Informatica Sistemi e Produzione
Università di Roma "Tor Vergata"
Via di Tor Vergata, 110, 00133 Roma (RM), Italy

Abstract—This paper describes a new numerical approach for the broad-band analysis of aperture antennas which avoids the use of both ω-domain and k-domain discrete Fourier transform. The FDTD method is adopted for the near field analysis of the antenna and the aperture field is then processed by time-domain modal expansion to obtain broadband gain pattern.

The new method is specified for rectangular aperture antennas and is demonstrated by means of some examples.

1. INTRODUCTION

Over the years, the Finite-Difference Time-Domain (FDTD) method has been widely used in the modelling of aperture-type antennas such as open-ended waveguides [1], horn antennas [2,3] and, more recently, cavity backed antennas [4,5]. The method has been applied both as a stand-alone tool and in combination with different numerical methods by domain decomposition. In the first case, the radiation pattern is generally obtained by the near-to-far field (N2F) transformation which requires the storage of equivalent electric and magnetic currents on a surface enclosing the whole geometry or, at least, on the antenna aperture. In this latter case, the simplified model of radiation from an aperture on a perfect ground is generally adopted [6]. N2F transformation procedures can be applied in both time and frequency domain. The first approach [7] is computationally intensive since equivalent sources must be processed at each time step and it is generally used to predict time-domain far field at a few points. Instead, to apply the N2F transformation in the frequency domain [8], the two-dimensional ω-domain discrete Fourier transform of the equivalent sources has to be available at each frequency point of interest. For this purpose, FDTD calculation has to be carried on until the complete transient damping [9]. This requirement usually yields long run-times especially in the analysis of waveguide antennas due to time domain oscillations of the waveguide modes at their own cut-off frequencies [10]. Also standard extrapolation techniques for transient signals [11] may not be utilized due to the high number of space samples of the equivalent sources involved in the N2F transformation. Finally, at each frequency point of interest a new N2F calculation is required without possibility to take advantage of any previously computed data. This fact limits a true broad-band computation of the radiation pattern leading to long run times. Above N2F transformation procedures will be hereafter referred to as *Total-N2F* since they operate on the equivalent total sources, as opposite to the method that will be described in this paper, which will be applied to a proper decomposition of the equivalent sources.

The present work aims at overcoming some of the drawbacks of Total-N2F by avoiding two-dimensional ω-domain discrete Fourier transform of the equivalent sources at each frequency of interest, and permits to speed-up the far field calculation by using closed form formula. The new approach is based on previous investigations over time domain modeling of waveguide modes by FDTD in combination with matrix methods and parameter estimation. In particular, in [12] a new algorithm has been proposed to model broad-band feed

antennas inside a waveguide region by the development of time-variant rectangular waveguide modal sources. Moreover, by a segmentation approach, the FDTD method has been hybridized [13] with the Generalized Admittance Matrix (GAM) method for application to corrugated horns with planar integrated sources. In this case the FDTD method is applied to the horn feeding region while the GAM method models the corrugations and the external radiation. A different hybrid procedure has been investigated in [14] for the analysis of emission from cavity backed apertures in EMC applications. The aperture field is calculated in the time domain by FDTD and expanded "at run-time" on suitable basis functions. The expansion coefficients are then processed in the time domain and extrapolation techniques are applied to speed up the numerical analysis. The external radiation is then obtained in the ω-domain by the Moment Method via an application of the Reciprocity Theorem. This strategy results in a mixed method which allows a partial data reusability.

In this paper, starting from a suitable time- and space-variable parametrization of the antenna aperture field computed by FDTD, a broad-band far field expression is derived analytically. The new method can be applied to model aperture antennas such as open-ended waveguides, horns and cavity backed antennas fed by any kind of launcher (coaxial probe, planar antenna).

The paper is organized as follows. The space- and time-domain modal parameter estimation of aperture field is first introduced and closed form expressions are given for broad-band far field computation in the case of rectangular apertures. Then, a numerical implementation is described with emphasis to the time-domain parametrization. Finally, some numerical calibrations are presented to discuss the accuracy of the method and its sensitivity to the parametrization order of the aperture field.

2. SPACE-TIME PARAMETRIZATION OF APERTURE FIELD

A waveguide is fed by a probe of arbitrarily geometrical shape, the voltage generator exciting the probe being an impulse-like signal $v_0(t)$ with limited bandwidth. The current flowing at the input terminals of the probe is denoted as $i_0(t)$.

The transverse electromagnetic field at any cross-section of the waveguide can be expressed in the time domain [12] by the following

expansion

$$\underline{E}_t(\underline{\rho}', z', t) \simeq \sum_{p=1}^{N} \underline{e}_p(\underline{\rho}') v_p(z', t) \tag{1}$$

where $\underline{\rho}' = x'\hat{x} + y'\hat{y}$ is a transverse vector on the waveguide cross-section S_a, $\{\underline{e}_p\}$ are time-independent TE and TM transverse waveguide eigenvectors with unitary normalization ($\int_{S_a} \underline{e}_p \cdot \underline{e}_q da' = \delta_{pq}$) and they are sorted in ascending order according to cut-off frequency (ω_p). The function $v_p(z', t)$ is the time-domain amplitude of the p-th mode and, by a proper normalization, has the meaning of time domain voltage on the equivalent transmission line for the p-th mode. The voltage v_p is related to the transverse field by the internal product:

$$v_p(z', t) = \int_{S_a} \underline{E}_t(\underline{\rho}', z', t) \cdot \underline{e}_p(\underline{\rho}') d\rho' \tag{2}$$

By consideration that, for an impulse like excitation signal $v_0(t)$, the modal voltage $v_p(z', t)$ is a damped oscillating signal [10], the well known complex exponential representation, [11, 15], can be used to expand v_p:

$$v_p(z', t) \simeq \sum_{k=-K_p}^{K_p} A_{pk}(z') e^{S_{pk}(z')t} \tag{3}$$

Complex poles $S_{pk}(z')$ and complex residues $A_{pk}(z')$ are generally dependent on the distance from the source plane and, since v_p is a real valued signal, they appear in conjugate pairs. The frequency domain counterparts of Eq. (1) is

$$\begin{aligned} \underline{E}_t(\underline{\rho}', z', \omega) &\simeq \sum_{p=1}^{N} \underline{e}_p(\underline{\rho}') V_p(z', \omega) \\ &\simeq \sum_{p=1}^{N} \underline{e}_p(\underline{\rho}') \sum_{k=-K_p}^{K_p} \frac{A_{pk}(z')}{j\omega - S_{pk}(z')} \end{aligned} \tag{4}$$

with $V_p(z', \omega) = \sum_{k=-K_p}^{K_p} \frac{A_{pk}(z')}{j\omega - S_{pk}(z')}$ is the Fourier transform of $v_p(z', t)$.

A similar representation holds for the magnetic field by means of the modal current $i_p(z', t)$.

If the waveguide is truncated (Fig. 1) and is let to radiate through the aperture S_A, it is worthwhile to adopt the same expansions of

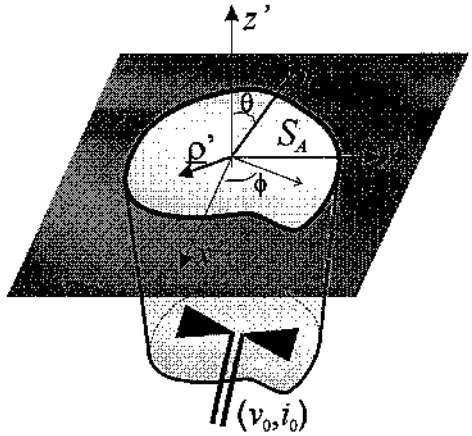

Figure 1. Coordinate systems for the open-ended waveguide problem. The shadowed bow-tie antenna is for a general purpose probe whose input port voltage and current are denoted by v_0 and i_0.

Eq. (1) and Eq. (4) for the electric field component laying onto the aperture, hereafter shortly denoted as $\underline{E}_a(\underline{\rho}', t)$. Aperture field is supposed to vanish everywhere else for $\underline{\rho}' \in S_a$ according to the well accepted model of aperture radiation from an infinite ground plane [6]. Although different kind of basis functions accounting for the aperture wedge effect are sometimes used, such as the spheroidal functions [6], nevertheless the waveguide transverse eigenvectors $\{\underline{e}_p\}$ have the attractive feature to form a vector basis and therefore a unique expansion coefficient v_p needs to be stored and processed for each ($e_{x,p}$, $e_{y,p}$) pair.

Voltage coefficients for aperture field expansion will be shortly denoted as $v_p(t)$ and residues and poles as a_{pk} and s_{pk}, respectively.

3. BROAD-BAND FAR FIELD COMPUTATION

The frequency domain far field radiated by the aperture on an infinite screen is calculated by the spectral domain method [16] in the asymptotic evaluation. This method is here generalized by means of broad-band modal expansion of the aperture field. The transverse component $\underline{f}_t$ of the *pattern space factor*, at any frequency ω, is here recalled to highlight the angular and frequency dependence:

$$\underline{f}_t(\theta, \phi, \omega) = \int_{S_A} \underline{E}_a(\underline{\rho}', \omega) e^{j\underline{k}_t(\theta,\phi,\omega)\cdot\underline{\rho}'} d\rho' \tag{5}$$

where $\underline{f}_t = f_x\hat{x} + f_y\hat{y}$, $\underline{k}_t = k_x\hat{x} + k_y\hat{y}$, $k_x = k_0 \sin\theta\cos\phi$, $k_0 \sin\theta \sin\phi, k_o = \omega/c$ and $d\rho' = dx'dy'$. Substitution of Eq. (4) in Eq. (5) gives the pattern space factor as summation of modal contributions, each weighted by the corresponding voltage coefficient:

$$\underline{f}_t(\theta,\phi,\omega) \simeq \sum_{p=1}^{N} V_p(\omega)\underline{F}_p(\theta,\phi,\omega) \tag{6}$$

Here, $\underline{F}_p$ (in m) is the *modal* pattern space factor corresponding to the p-th aperture mode:

$$\underline{F}_p(\theta,\phi,\omega) = \int_{S_A} \underline{e}_p(\underline{\rho}')e^{j\underline{k}_t(\theta,\phi,\omega)\cdot\underline{\rho}'}d\rho' \tag{7}$$

Denoting with $(E_{\theta,p},E_{\phi,p})$ the far field radiated by the $p-$th aperture mode with unitary excitation:

$$\begin{aligned} E_{\theta,p}(r,\theta,\phi,\omega) &= jk_0\frac{e^{-jk_0r}}{2\pi r}[F_{x,p}(\theta,\phi,\omega)\cos\phi + F_{y,p}(\theta,\phi,\omega)\sin\phi] \\ E_{\phi,p}(r,\theta,\phi,\omega) &= jk_0\frac{e^{-jk_0r}}{2\pi r}[F_{y,p}(\theta,\phi,\omega)\cos\phi - F_{x,p}(\theta,\phi,\omega)\sin\phi]\cos\theta \end{aligned} \tag{8}$$

the overall aperture-antenna far field can be finally computed as field superposition:

$$\begin{bmatrix} E_\theta(r,\theta,\phi,\omega) \\ E_\phi(r,\theta,\phi,\omega) \end{bmatrix} \simeq \sum_{p=1}^{N} \begin{bmatrix} E_{\theta,p}(r,\theta,\phi,\omega) \\ E_{\phi,p}(r,\theta,\phi,\omega) \end{bmatrix} \sum_{k=-K_p}^{K_p} \frac{a_{pk}}{j\omega - s_{pk}} \tag{9}$$

Eq. (9) gives the far field at any point and at any frequency ω within the spectrum bandwidth of the excitation signal v_0. Provided that the modal pattern space factors may be calculated in closed form, Eq. (9) allows any interesting far field function to be broadband computed without performing neither k-domain nor ω-domain discrete Fourier transforms of the FDTD-computed aperture field.

Since this method is based on the modal expansion of the aperture field, it will hereafter referred to as *Modal-N2F transformation.*

3.1. Computation of the Modal Pattern Space Factors

The proposed method is now specified to rectangular aperture antennas. The extension to circular aperture is straightforward.

For a rectangular aperture of $a \times b$ sides, the normalized TE_{mn} eigenvectors, expressed on a reference axis centered on the aperture left-down corner ($0 \leq x' \leq a$, $0 \leq y' \leq b$) are:

$$\begin{bmatrix} e^{TE}_{y,mn}(x',y') \\ e^{TE}_{z,mn}(x',y') \end{bmatrix} = T_{mn} \begin{bmatrix} k_n \cos(k_m x') \sin(k_n y') \\ -k_m \sin(k_m x') \cos(k_n y') \end{bmatrix} \tag{10}$$

$k_m = \frac{m\pi}{a}$, $k_n = \frac{n\pi}{b}$, $k_c = \sqrt{k_m^2 + k_n^2}$, $T_{mn} = \sqrt{\frac{2(1+\epsilon_{mn})}{ab}} \frac{1}{k_c}$ and $\epsilon_{mn} = 2$ or 4 if $m \cdot m = 0$ or $\neq 0$ respectively. The TM_{mn} functions are obtained from Eq. (10) with factors k_n and k_m replaced by $-k_m$ and k_n, respectively. Application of Eq. (7) requires the evaluation the following k-domain Fourier transforms:

$$\int \begin{bmatrix} \cos(k_m \xi) \\ \sin(k_m \xi) \end{bmatrix} e^{jk_\xi \xi} d\xi; \qquad \xi \in \{x', y'\} \tag{11}$$

Mathematical manipulations yield the following expressions for modal pattern space factors:

$$\begin{bmatrix} F^{TE}_{x,mn}(\theta,\phi,\omega) \\ F^{TE}_{y,mn}(\theta,\phi,\omega) \end{bmatrix} = \begin{bmatrix} k_n^2/k_y \\ -k_m^2/k_x \end{bmatrix} T_{mn} \varphi_{mn}(\theta,\phi,\omega) \tag{12}$$

with:

$$\varphi_{mn}(\theta,\phi,\omega) = 4k_x k_y (-j)^{m+n-1} \frac{\sin\left(\frac{k_x a + m\pi}{2}\right)}{k_m^2 - k_x^2} \frac{\sin\left(\frac{k_y b + n\pi}{2}\right)}{k_n^2 - k_y^2} \tag{13}$$

Similar expressions holds for TM modes with $F^{TM}_{x,mn} = -\frac{k_m}{k_n} F^{TE}_{x,mn}$ and $F^{TM}_{y,mn} = \frac{k_n}{k_m} F^{TE}_{y,mn}$.

3.2. Computation of the Antenna Gain

By simple algebraic manipulations, the radiation intensity can be expressed as

$$I(\theta,\phi,\omega) = \frac{k_0^2}{8\eta_0 \pi^2} [|f_x|^2 + |f_y|^2 - |f_x \sin\phi - f_y \cos\phi|^2 \sin^2\theta] \tag{14}$$

For the purpose of gain calculation, the antenna input power is evaluated at the antenna probe input port by the knowledge of port

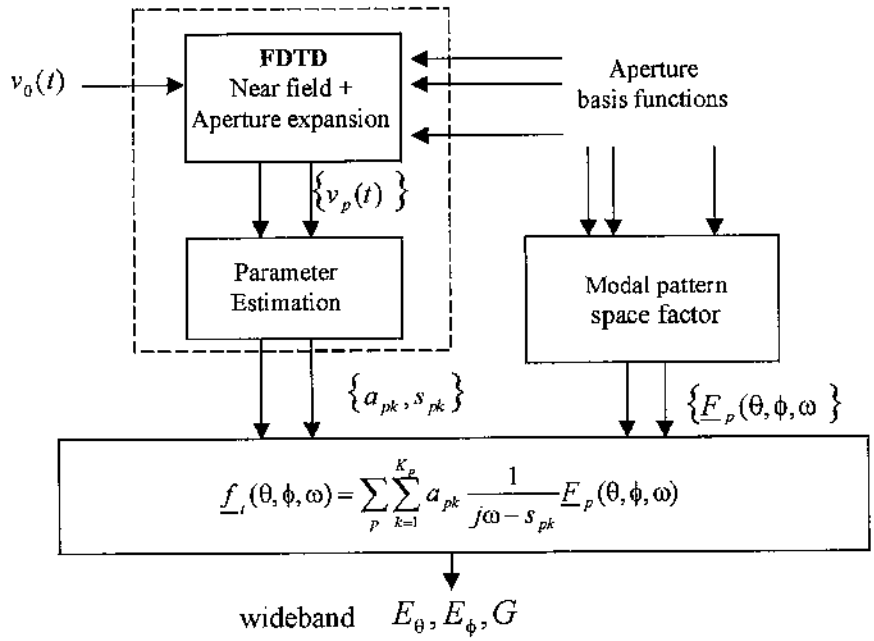

Figure 2. Flow-chart of the combined numerical/analytical procedure for the wideband computation of waveguide antenna pattern. Tasks within the dashed box are executed by Time Domain numerical algorithms.

voltage v_0 and current i_0:

$$P_{in}(\omega) = \mathrm{Re}\left(\frac{1}{2} V_0(\omega) I_0(\omega)^*\right) \tag{15}$$

with $I_0(\omega)$ and $V_0(\omega)$ the Fourier counterpart of $i_0(t)$ and $v_0(t)$.

4. METHOD IMPLEMENTATION

The computational steps involved in the application of the proposed method are summarized in Fig. 2. The tasks within the dashed box are executed by time domain algorithms. The FDTD solver preforms a fullwave analysis of the whole antenna including a small portion of the external free-space in the close surroundings of the aperture. In this case the computed aperture field will account for the wedge effect. The modal voltage coefficients $v_p(t)$ for the considered basis functions $\{\underline{e}_{pk}\}$

are computed "at run-time" by discretization of Eq. (2) on FDTD grid [12] at times $t_n = n\Delta t$, $(0 \leq t_n \leq N_t \Delta t)$.

The number of basis functions to be considered depends on the aperture discretization, on the maximum frequency and on the far field angular range of interest. According to investigations in [12] concerning the FDTD modelling of rectangular waveguide modes, the accuracy in the computation of voltage coefficient $v_p(t)$ is limited by the discrete approximation of the integral in Eq. (2) over the FDTD grid. It has been experimentally found that the (m,n)-modes, whose equivalent voltage is still computed with the typical FDTD accuracy is such that

$$m \leq \frac{a}{k\Delta} \qquad n \leq \frac{b}{k\Delta} \tag{16}$$

where $k = 15 - 20$ and a cubic FDTD grid, of cell size Δ, has been assumed.

The time signatures $v_p(t_n)$ are then used to estimate the parameters $\{a_{pk}, s_{pk}\}$ of each mode by the Matrix Pencil method [17]. First, the complex poles s_{pk} are estimated by means of Singular Value Decomposition. To prevent instabilities, the unstable poles $(\mathrm{Re}[s_{pk}] > 0)$ are pruned and the $2K_p'$ $(K_p' < K_p)$ residues a_{pk} are finally obtained from least square solution of the problem:

$$\begin{bmatrix} z_{p,-K_p'}^{(0)} & z_{p,-K_p'+1}^{(0)} & .. & z_{p,K_p'}^{(0)} \\ z_{p,-K_p'}^{(1)} & .. & .. & .. \\ .. & .. & .. & .. \\ z_{p,-K_p'}^{(N_t)} & z_{p,-K_p'+1}^{(N_t)} & & z_{p,K_p'}^{(N_t)} \end{bmatrix} \cdot \begin{bmatrix} a_{p,-K_p'} \\ a_{p,-K_p'+1} \\ .. \\ a_{p,K_p'} \end{bmatrix} = \begin{bmatrix} v_p(t_0) \\ v_p(t_1) \\ .. \\ v_p(t_{N_t}) \end{bmatrix} \tag{17}$$

with $z_{p,k}^{(n)} = e^{s_{pk} t_n}$.

The frequency domain spectra $V_p(\omega)$ are then available in analytical form at any desired frequency.

It is easily shown that the broadband aperture radiation is fully described by $4\sum_{p=0}^{N} K_p$ real valued parameters, with N the number of the considered aperture basis functions. Note that parameter estimation is performed once and for all and it is valid within the whole bandwidth of the excitation signal $v_0(t)$.

4.1. Numerical Complexity

The Modal N2F method is computationally more efficient than the traditional Total field transform. The numerical complexity of the two methods will be now compared in terms of multiplications. For

simplicity it is assumed that N_t is the number of FDTD time steps required by both methods to compute the aperture field. It is easily shown that the ratio (Speed Up) between the number of multiplications of Total-N2F and those of Modal-N2F is $SP \simeq [\frac{N}{2}(\frac{1}{N_f} + \frac{1}{N_c})]^{-1}$ where N_c is the number of FDTD cells on the aperture and N_f the number of the frequency samples. For typical geometries involving $N \simeq 10$, $N_f = 10^2$ and $N_c = 10^3$, a speed up in the CPU time of more than an order of magnitude is obtained.

5. NUMERICAL CALIBRATION

The method has been calibrated against two simple problems consisting of a flanged open-ended rectangular waveguide antenna and a rectangular pyramidal horn. Particular attention has been devoted to the number of modes required to have accurate far field outcomes.

The proprietary code BEST [18] has been used for FDTD simulations.

5.1. Open-Ended Waveguide

A rectangular open-ended waveguide is sourced by a coaxial probe and is provided with an external flange (Fig. 3). To better discuss the potentiality of the proposed method to deal with complex patterns, a metallic septum has been placed on the E-plane to excite higher order modes and therefore deform the radiation pattern.

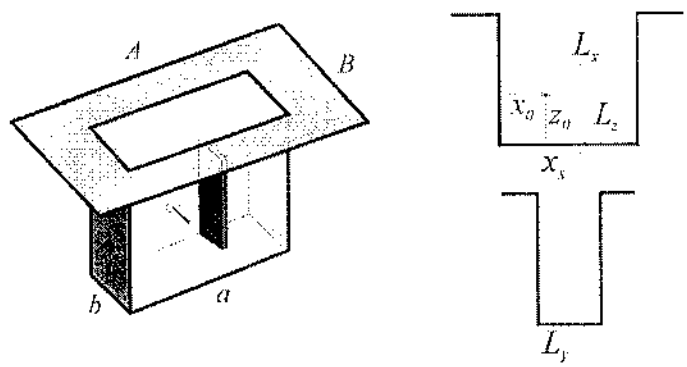

Figure 3. Open ended WR-90 waveguide antenna with flange and internal septum. Problem size (in mm): $x_0 = 7$, $y_0 = 19$, $z_0 = 7$ ($\lambda/4$ at 10 GHz), $L_x = 1.27$, $L_y = 6.35$, $L_z = 15$, $x_s = 13.3$, $a = 22.86$, $b = 10.16$, $h = 22.5$, $A = 39$, $B = 23$.

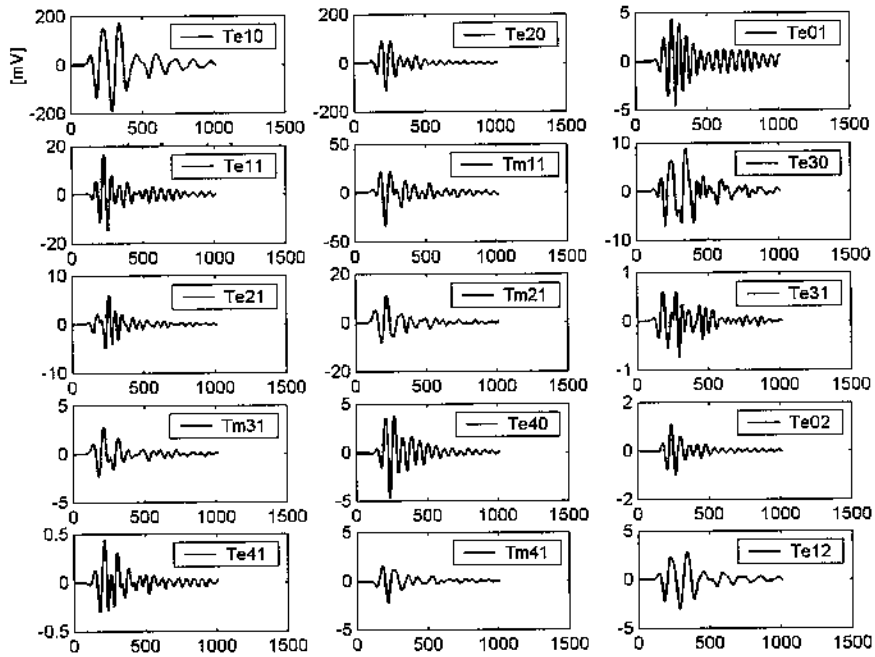

Figure 4. Modal voltages v_{mn} v.s. time (expressed in FDTD time steps) computed at the WR-90 open ended waveguide antenna.

The waveguide, a standard X band WR-90, has been meshed over a uniform grid with sizes $\Delta x = \Delta y = 0.635\,\text{mm}$, $\Delta z = 1\,\text{mm}$. The excitation voltage generator has been a gaussian signal $v_0(t) = v_g e^{-\frac{(t-\tau)^2}{2T^2}}$ with parameters τ and T such to give a 20% bandwidth of $[0, f_{\max} = 15GHz]$ ($V_0(f_{\max}) = 0.2V_0(0)$) and $v_g = 1V$. A reference solution has been obtained by the Total-N2F transformation which had to be repeated at each frequency point.

According to guidelines in Eq. (16) the maximum modal orders will be $m \leq 4$ and $n \leq 2$. Fifteen modal voltages $v_{mn}(t)$ have been therefore computed during FDTD calculation for the Modal-N2F transform method (see Tab. 1). Fig. 4 shows that TE_{10} and TE_{20} modes are excited at the highest extent, as expected by the waveguide discontinuities. Moreover, voltage amplitudes are strongly oscillating, and the FDTD simulation has therefore required long computation times to reach numerical convergence.

The E- and H-cuts of the normalized gain ($G/G_{\max}$), computed by the new method (15 modes) and the Total-N2F transformation,

Table 1. Modes for the WR-90 analysis ordered by the cut-off frequencies.

p	mode	cut − off[GHz]		p	mode	cut − off[GHz]
1	TE_{10}	6.55		9	TE_{31}	24.56
2	TE_{20}	13.10		10	TM_{31}	24.56
3	TE_{01}	14.73		11	TE_{40}	26.20
4	TE_{11}	16.13		12	TE_{02}	29.47
5	TM_{11}	16.13		13	TE_{41}	30.06
6	TE_{30}	19.65		14	TM_{41}	30.06
7	TE_{21}	10.72		15	TE_{12}	30.12
8	TM_{21}	19.72				

are compared in Fig. 5 at some frequencies. A good agreement can be appreciated both at lower frequency (8 GHz), where the only fundamental mode is really excited, and at higher frequencies where the main lobe shifts from the broadside (10 GHz) and a null occurs close to the broadside (12 GHz) due to the excitation of TE_{20}, TM_{11} and TM_{21} modes (labelled as $p = 2, 5$, and 8 respectively).

To investigate on the convergence of the modal expansion in the broadband far field computation, the following root mean square error (*r.m.s.*) has been computed for some frequencies:

$$\delta(\omega, N) = \frac{\left\| G(\theta, \phi, \omega, N) - \tilde{G}(\theta, \phi, \omega) \right\|_2}{\left\| \tilde{G}(\theta, \phi, \omega) \right\|_2} \tag{18}$$

where $G(\theta, \phi, N, \omega)$ is the gain computed with the Modal-N2F transformation by the use of the first N modes; $\tilde{G}$ is the gain obtained by the standard Total-N2F method and the norms $\| \circ \|$ are computed on the $0 \leq \theta \leq 90$ hemisphere by numerical discretization of integrals with form: $\|g(\theta, \phi)\|_2 = \sqrt{\int_0^{\pi} \int_{-\pi/2}^{\pi/2} |g(\theta, \phi)|^2 d\theta d\phi}$. The error at 8 GHz (see Fig. 6) is nearly insensible to the number of expansion modes, since the radiation pattern is mainly affected by the sole TE_{10} mode. Instead, the gain is computed with poor accuracy at higher frequencies if less than 4–5 modes are considered. The use of more than 6 modes does not further improve the accuracy.

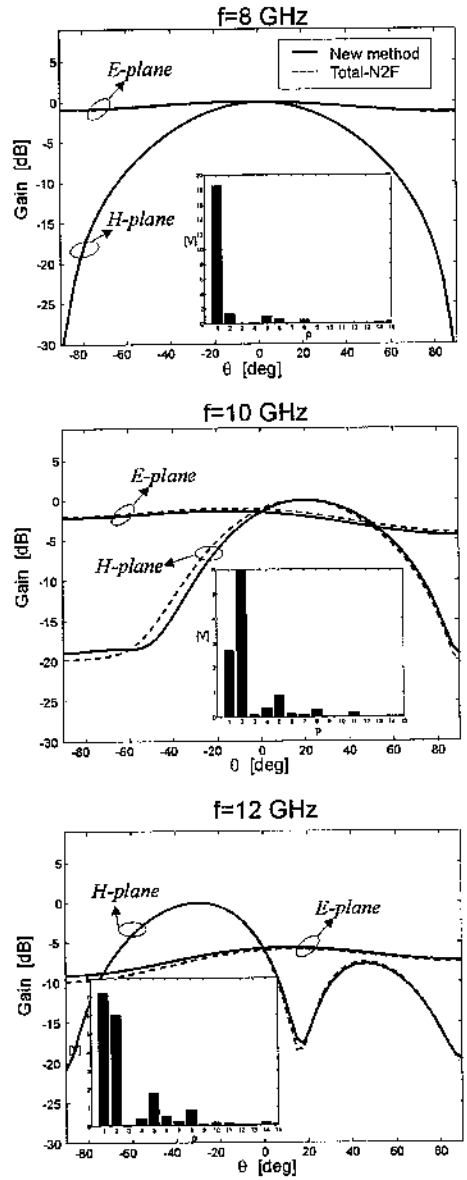

Figure 5. Normalised principal plane gain for the WR-90 waveguide antenna computed at some frequency points by the standard Total-N2F transform and the new method. The insets display the modal voltage amplitudes at each frequency.

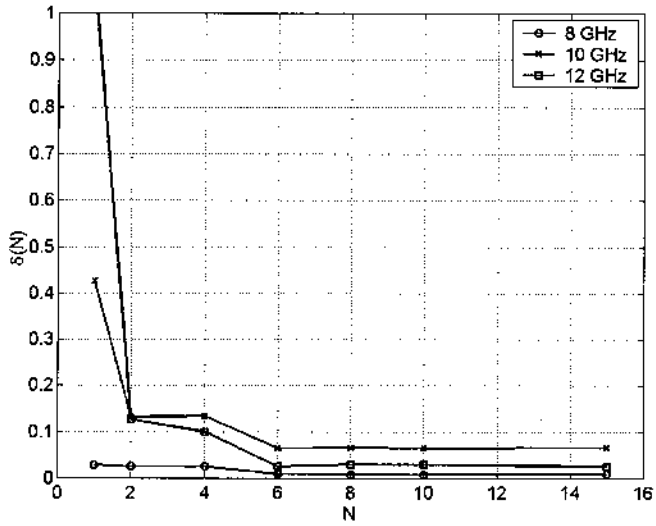

Figure 6. R.m.s. error in the WR-90 gain computation by new method for different numbers (N) of expansion modes.

5.2. Standard Gain Pyramidal Horn

A 20 dB pyramidal horn (X band) is connected to a WR-90 rectangular waveguide section (Fig. 7) which is in turn fed by a coaxial probe in the centre of E-plane. The structure has been meshed on a uniform grid with size $\Delta x = \Delta y = 1.27\,\text{mm}$ and $\Delta z = 2\,\text{mm}$. The simulation 20% bandwidth has been [0,15 GHz]. Because of the large size of the aperture, forty modes have been considered with cut-off frequency ranging from 1.20 GHz (TE_{10}) to 6.97 MHz (TE_{24}). The FDTD simulation has been turned off after 1500 time steps, when a steady state solution has occurred as it is required to apply the Total-N2F method for the calculation of the reference solution. Instead, only modal voltage samples in the first 800 time steps (Fig. 7b) have been used for parameter $\{a_{pk}, s_{pk}\}$ estimation.

Fig. 8 shows the normalized spectra of the modal voltages at 8, 10 and 12 GHz. It is worth noticing that at each frequency point only a few modal voltages are excited within three orders of magnitude respect to the highest voltage. To discuss the convergence of the gain pattern calculation against the number of modes, the computation of pattern space factor at any frequency $\tilde{\omega}$ (Eq. (6)) has been restricted to those N' modes, among the forty, whose amplitude $|V_q(\tilde{\omega})|$ is such that $|V_q(\tilde{\omega})|/|V_{\max}(\tilde{\omega})| \geq \varepsilon_t$, with ε_t is a threshold and $|V_{\max}(\tilde{\omega})|$ is the

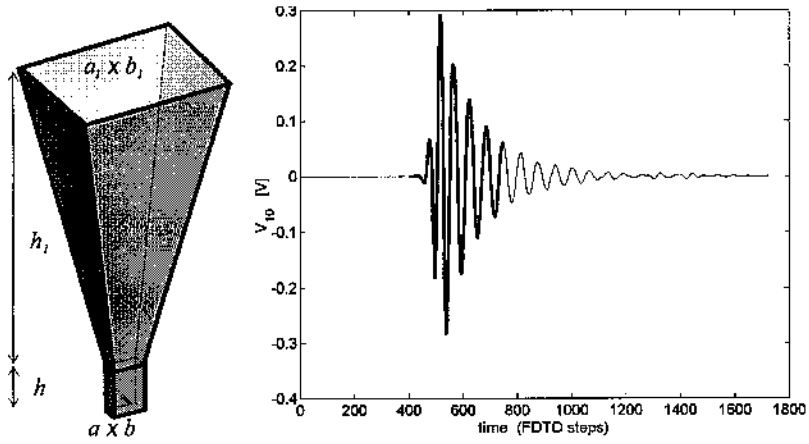

Figure 7. a) Standard-gain X-band horn antenna with sizes (in mm): $a_1 = 123.70$, $b_1 = 91.95$, $h_1 = 255.52$, $a = 22.86$, $b = 10.16$, $h = 21.50$; b) FDTD computed $v_{10}(t)$: in bold line the transient used for parameter estimation.

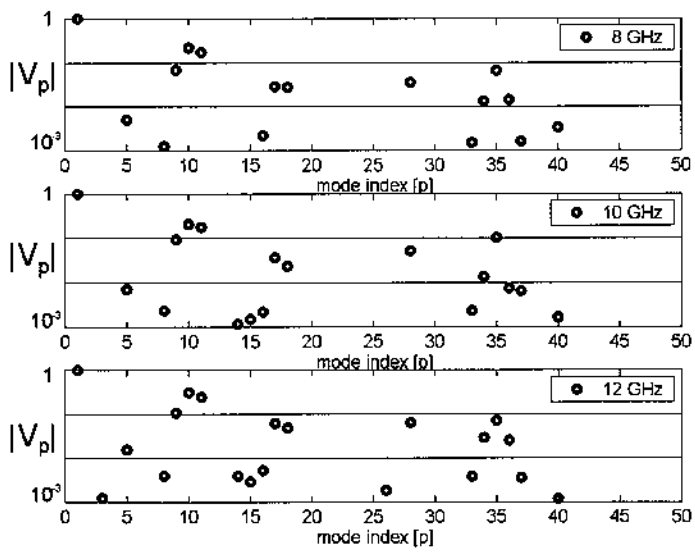

Figure 8. Normalized modal amplitudes $|V_p(f)|$ at 8, 10 and 12 GHz.

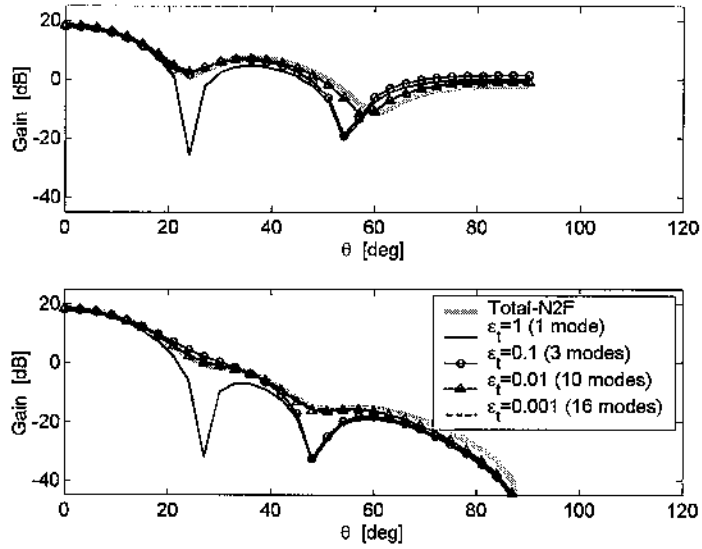

Figure 9. Convergence analysis: E- and H-plane at 8 GHz computed by the new method with different modal amplitude thresholds ε_t.

maximum among modal amplitudes at $\tilde{\omega}$. Fig. 9 to Fig. 11 report the 8, 10 and 12 GHz gain for $\varepsilon_t = \{1, 10^{-1}, 10^{-2}, 10^{-3}\}$. As expected, the number of basis functions, which are required for an accurate pattern prediction, increases with the frequency. In particular, a full agreement with the reference solution has been obtained at 8 GHz with not more than 10 modes ($\varepsilon_t = 10^{-2}$), whereas a less accurate prediction of the minima has been experienced at 10 GHz and 12 GHz even with the contribution of up to 20 modes ($\varepsilon_t = 10^{-3}$). More in detail, at 12 GHz the first null ($\theta \simeq 18°$) is correctly predicted by the use of only four modes ($\varepsilon_t = 10^{-1}$) whereas 11 modes ($\varepsilon_t = 10^{-2}$) must be considered for a good prediction of the second null ($\theta \simeq 30°$). Sharper nulls appear at $\theta \simeq 45°$ and at $\theta \simeq 65°$ due to the pedestal-like behavior of each aperture basis function which does not account for edge effects. Nevertheless the amplitude and the shape of sidelobes are correctly predicted all over the angular range.

As a further comparison the gain at 10 GHz on principal planes, as calculated by means of the Modal-N2F, has been superimposed to the corresponding curves obtained from measurements and simulations with different methods as they appear in [16] (see Fig. 12). It can be observed a good agreement especially in the H-plane, within the angular range $\pm 70°$ around the broadside.

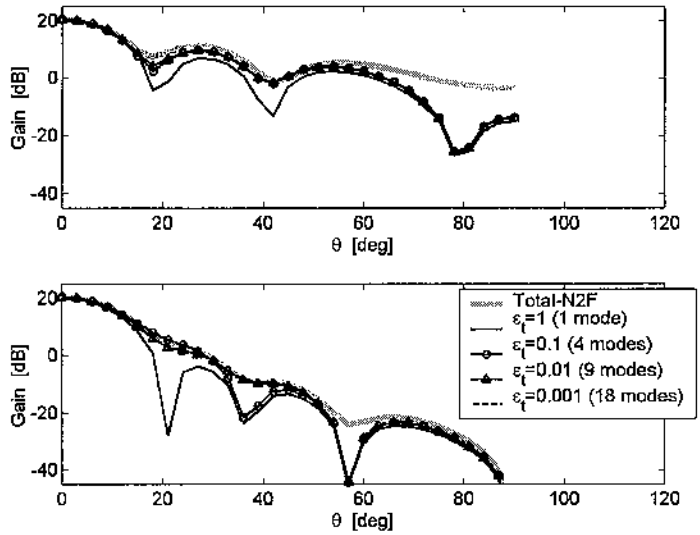

Figure 10. Convergence analysis: E- and H-plane at 10 GHz computed by the new method with different modal amplitude thresholds ε_t.

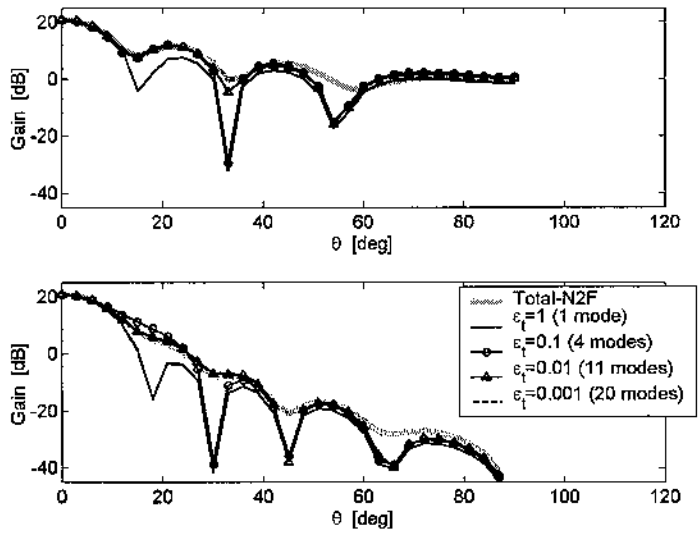

Figure 11. Convergence analysis: E- and H-plane at 12 GHz computed by the new method with different modal amplitude thresholds ε_t.

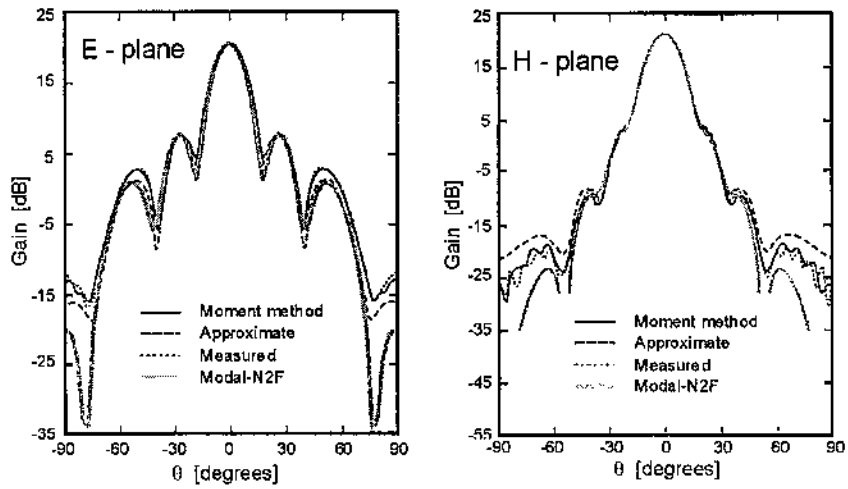

Figure 12. E- and H-plane gain at 10 GHz from the new method and from data in [16].

6. CONCLUSIONS

A new method has been proposed for the efficient calculation of far field radiated through aperture antennas. The method directly processes the time domain field which is FDTD-calculated on the aperture without the need of using neither discrete ω-domain nor k-domain Fourier transforms. As a consequence, the FDTD simulation can be terminated far before the steady state, provided that the electromagnetic response of the system is in the damping oscillating regime. A lot of CPU time can be therefore saved in comparison with standard near to far field transformations.

Numerical calibrations with realistic waveguide and horn antennas, have proved that few (6–10) modes, depending on the aperture electrical size, are enough to correctly predict the far field over a wide band.

A further benefit of the method is the possibility to evaluate the coupling among the antenna launcher and the aperture modes and to independently predict the contribution of each mode to far field radiation. These features permit the use of the proposed method in the design task when both the launcher and the waveguide/horn geometry need to be optimized.

ACKNOWLEDGMENT

This work has been partially supported by European Space Agency (ESTEC Contract 11476/95/NL/NB) and by the Ministero dell'Università e della Ricerca Scientifica (PRIN 2002).

The author wishes to thank Marco Sabbadini, Fernando Bardati and Piero Tognolatti for suggestions and helpful discussions.

REFERENCES

1. Katz, D. S., M. J. Piket-May, A. Taflove, and K. R. Umashankar, "FDTD analysis of electromagnetic wave radiation from systems containing horn antennas," *IEEE Trans. Antennas Propagat.*, Vol. 39, No. 8, 1203–1212, 1991.
2. Tirkas, P. A. and C. A. Balanis, "Finite-difference time-domain method for antenna radiation," *IEEE Trans. Antennas Propagat.*, Vol. 40, No. 3, 334–34, 1992.
3. Reig, C., E. A. Navarro, and V. Such, "FDTD analysis of E-sectoral horn antennas for broad-band applications," *IEEE Trans. Antennas Propagat.*, Vol. 45, No. 10, 14840-1487, 1997.
4. Omiya, M., T. Hikage, N. Ohno, K. Horiguchi, and K. Itoh, "Design of cavity-backed slot antennas using the finite-difference time-domain technique," *IEEE Trans. Antennas Propagat.*, Vol. 46, No. 12, 1853–1858, 1998.
5. Arakaki, D., D. H. Werner, and R. Mittra, "A technique for analyzing radiation from conformal antennas mounted on arbitrarily shaped conducting bodies," *J. of Electro. Waves and Appl.*, Vol. 14, No. 11, 1505–1523, 2000.
6. Rhodes, D. R., *Synthesis of Planar Antenna Sources*, Clarendon Press, Oxford, 1974.
7. Luebbers, R. J., K. S. Kunz, M. Schneider, and F. Hunsberger, "A finite-difference time-domain near zone to far zone transformation," *IEEE Trans. Antennas Propagat.*, Vol. 39, 429–433, 1991.
8. Taflove, A., *Computational Electrodynamics: The Finite Difference Time-Domain Method*, Artech House, Norwood, MA, 1995.
9. Marrocco, G. and F. Bardati, "Time-domain macromodel of planar microwave devices by FDTD and moment expansion," *IEEE Trans. Microwave Theory Tech.*, Vol. 49, 1321–1328, 2001.
10. Collin, R. E., *Field Theory of Guided Waves*, 535–, IEEE Press, Piscataway, NJ, 1991.
11. Poggio, A. J., M. L. Van Blaricum, E. K. Miller, and R. Mittra,

"Evaluation of a processing technique for transient data," *IEEE Trans. Antennas Propagat.*, Vol. 26, 165–173, Jan. 1978.

12. Marrocco, G. and F. Bardati, "Broadband horn-antenna launchers modelling by FDTD and generalized scattering matrix methods," to appear in *IEEE Trans. Antennas Propagat.*, October 2002.
13. Marrocco, G., A. Freni, L. Salghetti, and S. Maci, "A combined FDTD-GAM method for the modeling of rectangular corrugated horn fed by wide-band sources," *IEEE AP-S -International Symposium*, Vol. 4, 242–245, Boston, 2001.
14. Marrocco, G. and F. Bardati, "Combined time and frequency-domain modelling of electromagnetic radiation from apertures on resonant cavities by FDTD-MOM method," *J. of Electromagn. Waves and Appl.*, Vol. 16, No. 4, 523–539, 2002.
15. Baum, C. E., "Toward an engineering theory of electromagnetic scattering: the singularity and eigenmode expansion method," *Electromagnetic Scattering*, P. Uslenghi (ed.), 571–651, Academic Press, 1978.
16. Balanis, C., *Antenna Theory, Analysis and Design*, J. Wiley & Son, 1997.
17. Sarkar, T. K. and O. Pereira, "Using the matrix pencil method to estimate the parameters of a sum of complex exponential," *IEEE Antennas and Propagat. Magazine*, Vol. 37, No. 1, 48–55, 1995.
18. Marrocco, G. and F. Bardati, "BEST: a finite difference simulator for time electromagnetics," *Journal of Simulation Practice Theory*, No. 7, 279–293, 1999.

Gaetano Marrocco, Laurea in Electronic Engineering (1994), Ph.D. in Applied Electromagnetics (1998) both from University of LíAquila, Researcher and Assistant Professor at the University of Rome îTor Vergata since 1997. His research is mainly devoted to the development of numerical methods and signal processing techniques for the time domain modelling of complex electromagnetic structures in the context of biological and industrial applications.